Superconvergence of Local Discontinuous Galerkin Methods for Convection-Diffusion Equations

Yingda Cheng[a], Chi-Wang Shu[b,*]

[a] Department of Mathematics and ICES, University of Texas, Austin, TX 78712

[b] Division of Applied Mathematics, Brown University, Providence, RI 02912

Abstract

In this paper, we study the convergence behavior of the local discontinuous Galerkin (LDG) methods when applied to time dependent convection-diffusion equations. We show that the LDG solution will be superconvergent towards a particular projection of the exact solution, if this projection is carefully chosen based on the convection and diffusion fluxes. The order is observed to be at least $k + 2$ when piecewise P^k polynomials are used. Moreover, the numerical traces for the solution are also superconvergent, sometimes, of higher order. This is a continuation of our previous work [6], in which superconvergence of DG schemes for convection equations is discussed.

Keywords: local discontinuous Galerkin method; superconvergence; convection-diffusion equations; projection; error estimates.

*Corresponding author. Tel.: 1-401-863-2549; fax: 1-401-863-1355. E-mail: shu@dam.brown.edu.

1 Introduction

In this paper, we consider convection-diffusion equations

$$u_t + f(u,x)_x = (b(u)\, u_x)_x + c(x,t), \tag{1.1}$$

with $b(u) \geq 0$. We study the superconvergence behavior of the local discontinuous Galerkin (LDG) solution when the diffusion fluxes are taken as the alternating fluxes.

The discontinuous Galerkin (DG) method discussed here is a class of finite element methods using completely discontinuous piecewise polynomial space for the numerical solution and the test functions. It is originally devised to solve hyperbolic conservation laws containing only first order spatial derivatives, e.g. [10, 9, 8, 7, 11]. It has the advantage of flexibility for arbitrarily unstructured meshes, with a compact stencil, and with the ability to easily accommodate arbitrary *h*-*p* adaptivity. The DG method was later generalized to the LDG method by Cockburn and Shu to solve the convection-diffusion equation [12]. Their work was motivated by the successful numerical experiments of Bassi and Rebay [4] for the compressible Navier-Stokes equations.

In [6], we discussed the behavior of the error between the DG solution and the exact solution for conservation law problems. We showed that the DG solution is superconvergent toward a particular projection of the exact solution if upwind fluxes are used. Thus, the error will not grow for a long time. This work was motivated by [16], where the explicit formula of the DG solution is given by Fourier analysis, and [1, 3], where the superconvergence of the DG solutions at Radau points for ordinary differential equations is discussed.

For convection-diffusion equations, in [5], Celiker and Cockburn studied the steady state solution, and proved that for a large class of DG methods, the numerical traces are superconvergent. In [2], Adjerid and Klauser showed for convection or diffusion dominant time dependent equations, the LDG solution will be superconvergent at Radau points. However, they did not consider the general equation and the relation between the flux and superconvergence.

In this paper, we follow [6] and discuss the superconvergence property of the LDG scheme for convection-diffusion equations. We investigate the error of the LDG solution compared with the projection of the exact solution, as well as the error for the numerical traces. We prove the superconvergence result for the heat equation in the case of piecewise linear solutions, and give numerical tests to demonstrate the validity of the result for more general cases.

This paper is organized as follows: in Section 2, we review the LDG method for convection-diffusion equations. In Section 3, we prove that for P^1, the error between the LDG solution and a particular projection of the exact solution is superconvergent. In Section 4, we give numerical tests for linear and nonlinear equations to demonstrate the general validity of the superconvergence results. Finally, conclusions and future work are provided in Section 5.

2 The LDG method for convection-diffusion equations

In this section, we review the LDG method for convection-diffusion equations.

The convection-diffusion equations that we are interested in this paper are given as

$$\begin{cases} u_t + f(u,x)_x = (b(u)\, u_x)_x \\ u(x,0) = u_0(x) \\ u(0,t) = u(2\pi,t). \end{cases} \tag{2.1}$$

Here, $u_0(x)$ is a smooth 2π-periodic function and $b(u) \geq 0$.

The usual notation of the DG method is adopted. If we want to solve this equation on the interval $I = [a,b]$, first we divide it into N cells as follows

$$a = x_{\frac{1}{2}} < x_{\frac{3}{2}} < \ldots < x_{N+\frac{1}{2}} = b.$$

We denote

$$I_j = (x_{j-\frac{1}{2}}, x_{j+\frac{1}{2}}), \qquad x_j = \frac{1}{2}\left(x_{j-\frac{1}{2}} + x_{j+\frac{1}{2}}\right),$$

and $V_h^k = \{v : v|_{I_j} \in P^k(I_j),\ j = 1, \cdots, N\}$ to be the approximation space, where $P^k(I_j)$ denotes all polynomials of degree at most k on I_j. The LDG scheme is formulated based on rewriting (2.1) into

$$\begin{cases} u_t + f(u,x)_x - (a(u)q)_x = 0 \\ q - g(u)_x = 0, \end{cases} \tag{2.2}$$

with $a(u) = \sqrt{b(u)}$ and $g(u) = \int^u a(u)du$. Here, q is an auxiliary variable. Then the scheme becomes: find $u_h, q_h \in V_h^k$, such that

$$\int_{I_j} (u_h)_t v_h dx - \int_{I_j} f(u_h,x)(v_h)_x dx + \hat{f}(u_h,x)v_h^-|_{j+\frac{1}{2}} - \hat{f}(u_h,x)v_h^+|_{j-\frac{1}{2}}$$
$$+ \int_{I_j} a(u_h)q_h(v_h)_x dx - \hat{a}(u_h)\hat{q}_h v_h^-|_{j+\frac{1}{2}} + \hat{a}(u_h)\hat{q}_h v_h^+|_{j-\frac{1}{2}} = 0,$$
$$\int_{I_j} q_h w_h dx + \int_{I_j} g(u_h)(w_h)_x dx - \hat{g}(u_h)w_h^-|_{j+\frac{1}{2}} + \hat{g}(u_h)w_h^+|_{j-\frac{1}{2}} = 0$$

hold for any $v_h, w_h \in V_h^k$. Here and below $(v_h)^-_{j+\frac{1}{2}} = v_h(x^-_{j+\frac{1}{2}})$ denotes the left limit of the function v_h at the discontinuity point $x_{j+\frac{1}{2}}$. Likewise for v_h^+. $\hat{f}$ is a monotone numerical flux for the convection term [13]. $\hat{a}(u_h)$, $\hat{q}_h$ and $\hat{g}(u_h)$ are the diffusion fluxes, and are chosen using the criteria from [12]. For considerations of accuracy and compactness, in this paper, we will only consider the following alternating fluxes

$$\hat{q}_h = q_h^+, \qquad \hat{g}(u_h) = g(u_h^-), \qquad \hat{a}(u_h) = \frac{[g(u_h)]}{[u_h]}, \tag{2.3}$$

or

$$\hat{q}_h = q_h^-, \qquad \hat{g}(u_h) = g(u_h^+), \qquad \hat{a}(u_h) = \frac{[g(u_h)]}{[u_h]}, \tag{2.4}$$

where $[v_h] = v_h^+ - v_h^-$ denotes the jump of the function v_h at the cell interface. The numerical traces for the LDG scheme are defined as $\hat{f}(u_h, x) - \hat{a}(u_h)\hat{q}_h$ and $\hat{g}(u_h)$. They approximate $f(u, x) - a(u)q$ and $g(u)$, respectively.

In addition, we need to introduce two projections. $P_h^- u$ is defined in such a way that $P_h^- u \in V_h^k$,

$$\int_{I_j} P_h^- u\, v_h\, dx = \int_{I_j} u\, v_h\, dx$$

for any $v_h \in P^{k-1}$ on I_j and

$$(P_h^- u)^- = u^- \qquad \text{at } x_{j+1/2}.$$

Similarly, $P_h^+ u$ is defined in such a way that $P_h^+ u \in V_h^k$,

$$\int_{I_j} P_h^+ u\, v_h\, dx = \int_{I_j} u\, v_h\, dx$$

for any $v_h \in P^{k-1}$ on I_j and

$$(P_h^+ u)^+ = u^+ \qquad \text{at } x_{j-1/2}.$$

Notice that these special projections are used in the error estimates of the DG methods to derive optimal L^2 error bounds in the literature, e.g. in [17]. We are going to show that the numerical solution is closer to one of these two special projections of the exact solution than to the exact solution itself, depending on the choice of fluxes.

In the discussion that follows, we will consider various measurements of errors. Let us denote $e_u = u - u_h$ to be the error between the exact solution and the numerical solution, $\varepsilon_u = u - P_h u$ to be the projection error, and $\bar{e}_u = P_h u - u_h$ to be the error between the numerical solution and the projection of the exact solution. Similarly, for q, $e_q = q - q_h$ is the error between the exact solution and the numerical solution, $\varepsilon_q = q - P_h q$ is the projection error, and $\bar{e}_q = P_h q - q_h$ is the error between the numerical solution and the projection of the exact solution for q.

3 Proof for the P^1 LDG scheme solving the heat equation

In this section, we consider the heat equation when piecewise linear polynomials are used. Using the techniques in [15], we prove that $\bar{e}_u$ and $\bar{e}_q$ will achieve at least $(\frac{5}{2})$-th order (that is, $(k + \frac{3}{2})$-th order with $k = 1$) of superconvergence.

The heat equation is given by

$$\begin{cases} u_t - u_{xx} = 0 \\ u(x,0) = u_0(x) \\ u(0,t) = u(2\pi, t). \end{cases} \tag{3.5}$$

The LDG scheme is formulated based on rewriting (3.5) into

$$\begin{cases} u_t - q_x = 0 \\ q - u_x = 0. \end{cases} \tag{3.6}$$

Then the scheme becomes: find $u_h, q_h \in V_h^k$, such that

$$\begin{aligned} &\int_{I_j} (u_h)_t v_h dx + \int_{I_j} q_h (v_h)_x dx - \hat{q}_h v_h^-|_{j+\frac{1}{2}} + \hat{q}_h v_h^+|_{j-\frac{1}{2}} = 0, \\ &\int_{I_j} q_h w_h dx + \int_{I_j} u_h (w_h)_x dx - \hat{u}_h w_h^-|_{j+\frac{1}{2}} + \hat{u}_h w_h^+|_{j-\frac{1}{2}} = 0 \end{aligned} \tag{3.7}$$

hold for any $v_h, w_h \in V_h^k$. The alternating fluxes can be chosen as

$$(\hat{u}_h)_{j+\frac{1}{2}} = (u_h)^-_{j+\frac{1}{2}}, \quad (\hat{q}_h)_{j+\frac{1}{2}} = (q_h)^+_{j+\frac{1}{2}}, \tag{3.8}$$

or

$$(\hat{u}_h)_{j+\frac{1}{2}} = (u_h)^+_{j+\frac{1}{2}}, \quad (\hat{q}_h)_{j+\frac{1}{2}} = (q_h)^-_{j+\frac{1}{2}}. \tag{3.9}$$

Theorem 2.1. Let u, $q = u_x$ be the exact solution of the heat equation (3.5), and u_h, q_h be the LDG solution of (3.7). If the fluxes (3.8) are used, then we define $P_h u = P_h^- u$, $P_h q = P_h^+ q$, and we choose the initial condition as $u_h(\cdot, 0) = P_h^- u_0$. Otherwise, if the fluxes (3.9) are used, we let $P_h u = P_h^+ u$, $P_h q = P_h^- q$ and $u_h(\cdot, 0) = P_h^+ u_0$. In the case of P^1 elements and uniform meshes with mesh length equal to h, we have the following error estimate:

$$||\bar{e}_u(\cdot,t)||_{L^2} \le Ch^{5/2},$$

and

$$||\bar{e}_q(\cdot,t)||_{L^2} \le Ce^{-t}h^{5/2}$$

where C is a constant that does not depend on t or h.

Proof: We only prove for the flux choice (3.9). If we use (3.8), the proof is similar and is thus omitted. From (3.6), we have

$$\begin{aligned}
&\int_{I_j} u_t v_h dx + \int_{I_j} q(v_h)_x dx - q^- v_h^-|_{j+\frac{1}{2}} + q^- v_h^+|_{j-\frac{1}{2}} = 0, \\
&\int_{I_j} q w_h dx + \int_{I_j} u(w_h)_x dx - u^+ w_h^-|_{j+\frac{1}{2}} + u^+ w_h^+|_{j-\frac{1}{2}} = 0,
\end{aligned} \tag{3.10}$$

hold for any $v_h, w_h \in V_h^1$. Combined with (3.7), we have the error equations

$$\begin{aligned}
&\int_{I_j} (e_u)_t v_h dx + \int_{I_j} e_q(v_h)_x dx - e_q^- v_h^-|_{j+\frac{1}{2}} + e_q^- v_h^+|_{j-\frac{1}{2}} = 0, \\
&\int_{I_j} e_q w_h dx + \int_{I_j} e_u(w_h)_x dx - e_u^+ w_h^-|_{j+\frac{1}{2}} + e_u^+ w_h^+|_{j-\frac{1}{2}} = 0,
\end{aligned} \tag{3.11}$$

that hold for any $v_h, w_h \in V_h^1$. Taking $v_h = \bar{e}_u, w_h = \bar{e}_q$ and summing over j, we obtain

$$\int_I (\bar{e}_u)_t\, \bar{e}_u dx + \int_I (\bar{e}_q)^2 dx + \int_I (\varepsilon_u)_t\, \bar{e}_u dx + \int_I \varepsilon_q\, \bar{e}_q dx = 0.$$

Thus,

$$\frac{1}{2}\frac{d}{dt}||\bar{e}_u||_{L^2}^2 + \int_I (\bar{e}_q)^2 dx \le \left|\int_I (\varepsilon_u)_t\, \bar{e}_u dx\right| + \left|\int_I \varepsilon_q\, \bar{e}_q dx\right|. \qquad (3.12)$$

Next, we will perform a Fourier analysis on $\bar{e}_u$ and $\bar{e}_q$ to bound the right hand side of the above inequality. To simplify the discussion, we first take a single Fourier mode and assume $u_0(x) = \sin(x)$. In this case, we know the exact solution of (3.5) is $u(x,t) = e^{-t}\sin(x)$ and $q(x,t) = e^{-t}\cos(x)$. Hence, we can compute the projection of u to be

$$P_h^+ u = c_j + d_j \frac{x - x_j}{h}, \qquad P_h^- q = a_j + b_j \frac{x - x_j}{h}$$

on I_j, where $c_j = \frac{e^{-t}}{h}(-\cos(x_{j+\frac{1}{2}}) + \cos(x_{j-\frac{1}{2}}))$, $d_j = 2(c_j - e^{-t}\sin(x_{j-\frac{1}{2}}))$; $a_j = \frac{e^{-t}}{h}(\sin(x_{j+\frac{1}{2}}) - \sin(x_{j-\frac{1}{2}}))$, and $b_j = 2(e^{-t}\cos(x_{j+\frac{1}{2}}) - a_j)$. On the other hand, the numerical solution u_h can be expressed in the following form

$$u_h|_{I_j} = u_{j-\frac{1}{4}}\phi_{j-\frac{1}{4}}(x) + u_{j+\frac{1}{4}}\phi_{j+\frac{1}{4}},$$

$$q_h|_{I_j} = q_{j-\frac{1}{4}}\phi_{j-\frac{1}{4}}(x) + q_{j+\frac{1}{4}}\phi_{j+\frac{1}{4}},$$

where $\phi_{j-\frac{1}{4}}(x) = \frac{2}{h}(x_{j+\frac{1}{4}} - x)$ and $\phi_{j+\frac{1}{4}}(x) = \frac{2}{h}(x - x_{j-\frac{1}{4}})$ are the basis functions. The values of $u_{j\pm\frac{1}{4}}$ can be obtained using the techniques in [15] as

$$
\begin{aligned}
u_{j-\frac{1}{4}} &= e^{-t}\left(\sin(x_j) - \tfrac{h}{4}\cos(x_j) - \tfrac{7h^2}{96}\sin(x_j) + \tfrac{17h^3}{1152}\cos(x_j)\right) + O(h^4),\\
u_{j+\frac{1}{4}} &= e^{-t}\left(\sin(x_j) + \tfrac{h}{4}\cos(x_j) + \tfrac{h^2}{96}\sin(x_j) + \tfrac{5h^3}{384}\cos(x_j)\right) + O(h^4),\\
q_{j-\frac{1}{4}} &= e^{-t}\left(\cos(x_j) + \tfrac{h}{4}\sin(x_j) + \tfrac{h^2}{96}\cos(x_j) - \tfrac{h^3}{1152}\sin(x_j)\right) + O(h^4),\\
q_{j+\frac{1}{4}} &= e^{-t}\left(\cos(x_j) - \tfrac{h}{4}\sin(x_j) - \tfrac{7h^2}{96}\cos(x_j) + \tfrac{h^3}{1152}\sin(x_j)\right) + O(h^4).
\end{aligned}
$$

After a Taylor expansion, we have

$$
\begin{aligned}
\bar{e}_u &= -e^{-t}\left(\frac{1}{72} + \frac{11}{288}\frac{x-x_j}{h}\right)\cos(x_j)h^3 + O(h^4)\\
\bar{e}_q &= -\frac{e^{-t}}{96}\cos(x_j)h^2 + e^{-t}\frac{11}{288}\frac{x-x_j}{h}\sin(x_j)h^3 + O(h^4) \qquad \text{on } I_j.
\end{aligned}
$$

By similar arguments, we can prove that if $u_0(x) = \sin(kx)$, then

$$
\begin{aligned}
\bar{e}_u &= -e^{-k^2t}\left(\frac{1}{72} + \frac{11}{288}\frac{x-x_j}{h}\right)\cos(kx_j)k^3h^3 + O((kh)^4),\\
\bar{e}_q &= -\frac{e^{-k^2t}}{96}\cos(kx_j)k^2h^2 + e^{-k^2t}\frac{11}{288}\frac{x-x_j}{h}\sin(kx_j)k^3h^3 + O((kh)^4) \qquad \text{on } I_j.
\end{aligned}
$$

and if $u_0(x) = \cos(kx)$, then

$$
\begin{aligned}
\bar{e}_u &= e^{-k^2t}\left(\frac{1}{72} + \frac{11}{288}\frac{x-x_j}{h}\right)\sin(kx_j)k^3h^3 + O((kh)^4),\\
\bar{e}_q &= \frac{e^{-k^2t}}{96}\sin(kx_j)k^2h^2 + e^{-k^2t}\frac{11}{288}\frac{x-x_j}{h}\cos(kx_j)k^3h^3 + O((kh)^4) \qquad \text{on } I_j.
\end{aligned}
$$

For any smooth initial condition $u_0(x)$, the Fourier series of u_0 is

$$u_0(x) = \frac{1}{2}b_0 + \sum_{k=1}^{\infty}[a_k \sin(kx) + b_k \cos(kx)]$$

where $a_k = \frac{1}{\pi}\int_0^{2\pi} u_0(x)\sin(kx)dx$, and $b_k = \frac{1}{\pi}\int_0^{2\pi} u_0(x)\cos(kx)dx$. Then,

$$q_0 = (u_0)_x = \sum_{k=1}^{\infty}[a_k k \cos(kx) - b_k k \sin(kx)],$$

and the exact solution to (3.5) is

$$u(x,t) = \frac{1}{2}b_0 + \sum_{k=1}^{\infty} e^{-k^2 t}[a_k \sin(kx) + b_k \cos(kx)],$$
$$q(x,t) = \sum_{k=1}^{\infty} e^{-k^2 t}[a_k k \cos(kx) - b_k k \sin(kx)].$$

It is well known that

$$a_k, b_k = O\left(\frac{1}{k^p}\right) \tag{3.13}$$

if $u_0 \in C^p$.

Since P_h^- and P_h^+ are linear operators,

$$P_h^+ u(x,t) = \frac{1}{2}b_0 + \sum_{k=1}^{\infty} e^{-k^2 t}[a_k P_h^+ \sin(kx) + b_k P_h^+ \cos(kx)],$$
$$P_h^- q(x,t) = \frac{1}{2}b_0 + \sum_{k=1}^{\infty} e^{-k^2 t}[a_k k P_h^- \cos(kx) - b_k k P_h^- \sin(kx)].$$

We can also prove by the dominated convergence theorem that

$$u_h(x,t) = \frac{1}{2}b_0 + \sum_{k=1}^{\infty}[a_k u_h^k(x,t) + b_k w_h^k(x,t)],$$
$$q_h(x,t) = \sum_{k=1}^{\infty}[a_k q_h^k(x,t) + b_k v_h^k(x,t)],$$

where $u_h^k(x,t)$ and $q_h^k(x,t)$ are the LDG solution to

$$\begin{cases} u_t - u_{xx} = 0 \\ u(x,0) = \sin(kx) \\ u(0,t) = u(2\pi,t), \end{cases}$$

and $w_h^k(x,t)$, $v_h^k(x,t)$ are the LDG solution to

$$\begin{cases} u_t - u_{xx} = 0 \\ u(x,0) = \cos(kx) \\ u(0,t) = u(2\pi,t). \end{cases}$$

Thus, if $p \geq 6$, we have

$$\begin{aligned} \bar{e}_u \;\; = \;\; & \sum_{k=1}^{\infty} \frac{e^{-k^2 t}}{72}[-a_k \cos(kx_j) + b_k \sin(kx_j)]k^3 h^3 \\ & + \sum_{k=1}^{\infty} e^{-k^2 t}\frac{11}{288}[-a_k \cos(kx_j) + b_k \sin(kx_j)]\frac{x - x_j}{h}k^3 h^3 + O(h^4) \end{aligned}$$

and

$$\bar{e}_q = \sum_{k=1}^{\infty} \frac{e^{-k^2 t}}{96}[-a_k \cos(kx_j) + b_k \sin(kx_j)]k^2 h^2$$
$$+ \sum_{k=1}^{\infty} e^{-k^2 t} \frac{11}{288}[a_k \sin(kx_j) + b_k \cos(kx_j)] \frac{x - x_j}{h} k^3 h^3 + O(h^4)$$

By the properties of the projection P_h^-, we know that on I_j

$$\int_{I_j} (\varepsilon_u)_t \, dx = 0, \qquad \int_{I_j} \varepsilon_q \, dx = 0$$

and $(\varepsilon_q)_t \leq C_1 e^{-t} h^2$, $(\varepsilon_u)_t \leq C_1 e^{-t} h^2$ where the constant C_1 does not depend on t or h. Moreover, by (3.13) with $p \geq 5$, there exists C_2, such that

$$\left| \sum_{k=1}^{\infty} e^{-(k^2-1)t} \frac{11}{288}[-a_k \cos(kx_j) + b_k \sin(kx_j)]k^3 \right| \leq C_2$$

and

$$\left| \sum_{k=1}^{\infty} e^{-(k^2-1)t} \frac{11}{288}[a_k \sin(kx_j) + b_k \cos(kx_j)]k^3 \right| \leq C_2$$

for all j. Thus,

$$\left| \int_{I_j} (\varepsilon_u)_t \, \bar{e}_u dx \right| \leq 2C_1 C_2 e^{-2t} h^6$$

and

$$\left| \int_{I_j} \varepsilon_q \, \bar{e}_q dx \right| \leq 2C_1 C_2 e^{-2t} h^6$$

if h is small enough. Summing over j and using (3.12), we obtain

$$\frac{1}{2}\frac{d}{dt}||\bar{e}_u||^2_{L^2} + \int_I (\bar{e}_q)^2 dx \le 4C_1C_2e^{-2t}h^5.$$

Thus, we have proved

$$||\bar{e}_u(\cdot,t)||_{L^2} \le Ch^{5/2},$$

and

$$||\bar{e}_q(\cdot,t)||_{L^2} \le Ce^{-t}h^{5/2}.$$

■

4 Numerical test for the general cases

In this section, we test various numerical examples to show that our conclusion holds true for very general cases. To make the temporal error negligible compared to the spatial error in the numerical tests, we use the third order TVD Runge-Kutta time stepping [14] with $\triangle t = CFL\triangle x^4$, with CFL small enough. We do not discuss the influence of the time discretization error in this paper.

4.1 Linear equations with constant coefficients

In this subsection, linear equations with constant coefficients are discussed. We test the heat equation, a convection-diffusion equation with equal coefficients for convection and diffusion, and a convection-dominated convection-diffusion equation.

Example 1. We solve the heat equation

$$\begin{cases} u_t = u_{xx} \\ u(x,0) = \sin(x) \\ u(0,t) = u(2\pi,t). \end{cases}$$

The exact solution to this problem is

$$u(x,t) = e^{-t}\sin(x).$$

We use the alternating fluxes (3.8). According to this flux choice, the projections for u and q are chosen as $P_h^- u$ and $P_h^+ q$ respectively.

Tables 4.2 to 4.4 list the numerical errors and their orders when $k \geq 1$. In addition to e_u, $\bar{e}_u$, e_q and $\bar{e}_q$, we also list the point errors for the right end points for u and the left end points for q, namely, $e_u^-(x_{j+1/2})$ and $e_q^+(x_{j-1/2})$. These are the errors for the two numerical traces u_h^- and q_h^+. We observe that while $\bar{e}_u$ and $\bar{e}_q$ achieve $(k+2)$-th order superconvergence, errors for the numerical traces in general have order greater than or equal to $(k+2)$.

For P^0, the projections P_h^+ and P_h^- can no longer be defined, so we only list e and q and some point errors in Table 4.1. From our observation, unlike for the other cases, superconvergence is achieved at the midpoints for u and at the left end points for q.

If we pick the fluxes as in (3.9), the conclusions are similar and are thus omitted here.

Table 4.1: Example 1 when using P^0 polynomials on a uniform mesh of N cells. $T = 1$.

	e_u		$e_u(x_j)$	
N	L^2 error	order	L^2error	order
10	4.76E-02	-	4.19E-03	-
20	2.36E-02	1.01	1.06E-03	1.98
40	1.18E-02	1.00	2.67E-04	1.99
80	5.90E-03	1.00	6.68E-05	2.00
160	2.95E-03	1.00	1.67E-05	2.00
	e_q		$e_q^+(x_{j-1/2})$	
10	1.55E-01	-	1.20E-03	-
20	4.71E-02	0.99	1.93E-04	2.64
40	2.36E-02	1.00	8.22E-06	4.55
80	1.02E-02	1.00	1.02E-07	6.33
160	5.90E-03	1.00	9.63E-09	3.41

In Theorem 2.1 we have proved that the error $\bar{e}_q$ decays exponentially with respect to time. In fact, our numerical results show that all the aforementioned errors decay exponentially with respect to time, see Figure 4.1.

The proof of superconvergence in Theorem 2.1 uses Fourier analysis and is thus restricted to uniform meshes. However, our numerical experiments indicate that the superconvergence result holds also for non-uniform meshes. In 4.5, we list the errors and orders for a non-uniform mesh which is a 10% random perturbation of the uniform mesh. We can see that all the conclusions for uniform meshes also hold true for this non-uniform mesh.

Table 4.2: Example 1 when using P^1 polynomials on a uniform mesh of N cells. $T = 1$.

	e_u		$\bar{e}_u$		$e_u^-(x_{j+1/2})$	
N	L^2 error	order	L^2 error	order	L^2error	order
10	6.28E-03	-	1.04E-03	-	9.82E-05	-
20	1.56E-03	2.01	1.29E-04	3.00	5.93E-06	4.05
40	3.91E-04	2.00	1.62E-05	3.00	3.68E-07	4.01
80	9.77E-05	2.00	2.02E-06	3.00	2.29E-08	4.00
	e_q		$\bar{e}_q$		$e_q^+(x_{j-1/2})$	
10	6.35E-03	-	5.32E-04	-	9.22E-04	-
20	1.57E-03	2.02	6.51E-05	3.03	1.13E-04	3.03
40	3.91E-04	2.00	8.10E-06	3.01	1.40E-05	3.01
80	9.77E-05	2.00	1.01E-06	3.00	1.75E-06	3.00

Example 2. We solve the convection-diffusion equation

$$\begin{cases} u_t + u_x = u_{xx} \\ u(x,0) = \sin(x) \\ u(0,t) = u(2\pi,t). \end{cases}$$

The exact solution to this problem is

$$u(x,t) = e^{-t}\sin(x-t).$$

We use the upwind flux u_h^- for the convective term, and the alternating fluxes (3.8) for the diffusion. Notice that this choice of the diffusive fluxes is consistent with the convective flux, namely the flux for u_h are chosen as u_h^- for both the convective and the diffusive terms. The projection for u is

Table 4.3: Example 1 when using P^2 polynomials on a uniform mesh of N cells. $T = 1$.

	e_u		$\bar{e}_u$		$e_u^-(x_{j+1/2})$	
N	L^2 error	order	L^2 error	order	L^2error	order
10	3.15E-04	-	2.53E-05	-	3.62E-06	-
20	3.94E-05	3.00	1.55E-06	4.03	1.11E-07	5.03
40	4.92E-06	3.00	9.65E-08	4.01	3.46E-09	5.01
80	6.15E-07	3.00	6.03E-09	4.00	1.08E-10	5.00
	e_q		$\bar{e}_q$		$e_q^+(x_{j-1/2})$	
10	3.15E-04	-	2.51E-05	-	4.73E-07	-
20	3.94E-05	3.00	1.55E-06	4.02	8.29E-09	5.84
40	4.92E-06	3.00	9.65E-08	4.00	8.90E-11	6.54
80	6.15E-07	3.00	6.03E-09	4.00	1.17E-12	6.25

chosen as P_h^-, while the projection for q is P_h^+.

Tables 4.6 to 4.8 list the numerical errors and their orders. Similar superconvergence is observed as in Example 1. We have $(k+2)$-th order for $\bar{e}_u$ and $\bar{e}_q$ and at least $(k+2)$-th order for the point errors. Note that in this case, the numerical traces are $u_h^- - q_h^+$ and u_h^-, so the results imply the superconvergence for the numerical traces.

We now use (3.9) as the diffusion fluxes and define the projection for u as P_h^+. Notice that this choice of the diffusive fluxes is inconsistent with the convective flux, namely the flux for u_h are chosen as u_h^+ for the diffusive flux and as u_h^- for the convective flux. In this case, the numerical traces are $u^- - q^-$ and u^+. Let us define $w = u - q$ and denote $\bar{e}_w$ as the difference between w and $P_h^- w$. From Tables 4.9 to 4.11, we clearly observe superconvergence for the two numerical traces as well as for $P_h^+ u$ and $P_h^- w$. Therefore, the

Table 4.4: Example 1 when using P^3 polynomials on a uniform mesh of N cells. $T = 1$.

	e_u		$\bar{e}_u$		$e_u^-(x_{j+1/2})$	
N	L^2 error	order	L^2 error	order	L^2error	order
5	1.93E-04	-	2.08E-05	-	1.78E-07	-
10	1.21E-05	3.99	6.37E-07	5.03	5.15E-10	8.43
20	7.60E-07	4.00	1.98E-08	5.01	2.13E-12	7.92
	e_q		$\bar{e}_q$		$e_q^+(x_{j-1/2})$	
5	1.93E-04	-	2.08E-05	-	1.02E-06	-
10	1.21E-05	3.99	6.37E-07	5.03	7.31E-09	7.13
20	7.60E-07	4.00	1.98E-08	5.01	5.60E-11	7.03

superconvergence results are not dependent upon whether the diffusion fluxes are chosen to be consistent with the convective flux, as long as we interpret the correct quantities to look for superconvergence.

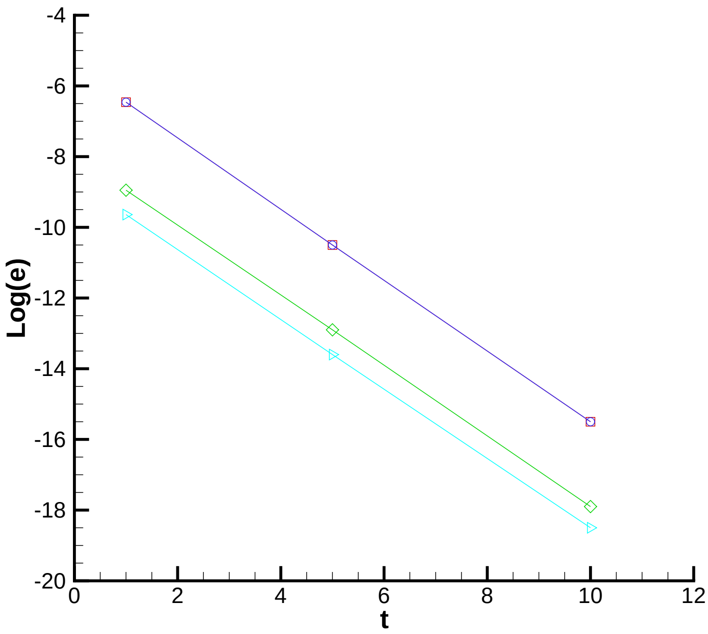

Figure 4.1: Example 1, errors versus time when using P^1 polynomials on a uniform mesh of 20 cells. Squares: e_u; Diamonds: $\bar{e}_u$; Circles: e_q; Right Triangles: $\bar{e}_q$.

Table 4.5: Example 1 when using P^1 polynomials on a random mesh of N cells. $T = 1$.

	e_u		$\bar{e}_u$		$e_u^-(x_{j+1/2})$	
N	L^2 error	order	L^2 error	order	L^2error	order
10	6.94E-03	-	1.02E-03	-	1.81E-04	-
20	1.61E-03	2.10	1.43E-04	2.84	9.52E-06	4.25
40	4.07E-04	1.99	1.76E-05	3.02	6.53E-07	3.87
80	1.09E-04	1.90	2.30E-06	2.94	4.20E-08	3.96
	e_q		$\bar{e}_q$		$e_q^+(x_{j-1/2})$	
10	6.15E-03	-	6.97E-04	-	1.05E-03	-
20	1.64E-03	1.90	7.66E-05	3.19	1.18E-04	3.15
40	4.07E-04	2.01	9.57E-06	3.00	1.47E-05	3.00
80	1.09E-04	1.90	1.23E-06	2.96	1.97E-06	2.90

Table 4.6: Example 2 when using P^1 polynomials on a uniform mesh of N cells. $T = 1$. The diffusion fluxes are chosen as (3.8).

	e_u		$\bar{e}_u$		$e_u^-(x_{j+1/2})$	
N	L^2 error	order	L^2 error	order	L^2error	order
10	6.33E-03	-	1.18E-03	-	1.01E-03	-
20	1.57E-03	2.01	1.59E-04	2.90	1.19E-04	3.09
40	3.91E-04	2.00	2.06E-05	2.95	1.44E-05	3.04
80	9.77E-05	2.00	2.62E-06	3.00	1.77E-06	3.02
	e_q		$\bar{e}_q$		$e_q^+(x_{j-1/2})$	
10	5.69E-03	-	1.40E-03	-	1.06E-03	-
20	1.48E-03	1.95	1.78E-04	2.98	1.64E-04	2.88
40	3.79E-04	1.96	2.25E-05	2.98	1.89E-05	2.93
80	9.61E-05	1.98	2.84E-06	2.99	2.42E-06	2.97

Table 4.7: Example 2 when using P^2 polynomials on a uniform mesh of N cells. $T = 1$. The diffusion fluxes are chosen as (3.8).

	e_u		$\bar{e}_u$		$e_u^-(x_{j+1/2})$	
N	L^2 error	order	L^2 error	order	L^2error	order
10	3.15E-04	-	2.07E-05	-	4.48E-06	-
20	3.94E-05	3.00	1.40E-06	3.89	1.48E-07	4.92
40	4.92E-06	3.00	9.17E-08	3.93	4.75E-09	4.96
80	6.15E-07	3.00	5.87E-09	3.96	1.51E-10	4.98
	e_q		$\bar{e}_q$		$e_q^+(x_{j-1/2})$	
10	2.94E-04	-	5.40E-05	-	8.29E-06	-
20	3.80E-05	2.95	3.41E-06	3.99	2.51E-07	5.05
40	4.83E-06	2.97	2.14E-07	3.99	7.77E-09	5.01
80	6.09E-07	2.99	1.34E-08	4.00	2.42E-10	5.00

Table 4.8: Example 2 when using P^3 polynomials on a uniform mesh of N cells. $T = 1$. The diffusion fluxes are chosen as (3.8).

	e_u		$\bar{e}_u$		$e_u^-(x_{j+1/2})$	
N	L^2 error	order	L^2 error	order	L^2error	order
5	1.93E-04	-	1.52E-05	-	2.38E-06	-
10	1.21E-05	3.99	5.49E-07	4.79	1.66E-08	7.16
20	7.60E-07	4.00	1.84E-08	4.90	1.26E-10	7.05
40	4.75E-08	4.00	5.98E-10	4.95	1.98E-12	5.99
	e_q		$\bar{e}_q$		$e_q^+(x_{j-1/2})$	
5	1.76E-04	-	4.37E-05	-	1.05E-06	-
10	1.16E-05	3.92	1.39E-06	4.97	8.61E-09	6.93
20	7.41E-07	3.96	4.39E-08	4.99	7.32E-11	6.88
40	4.69E-08	3.98	1.38E-09	4.99	4.36E-13	7.39

Table 4.9: Example 2 when using P^1 polynomials on a uniform mesh of N cells. $T = 1$. The diffusion fluxes are chosen as (3.9).

	e_u		$\bar{e}_u$		$e_u^+(x_{j-1/2})$	
N	L^2 error	order	L^2 error	order	L^2error	order
10	5.65E-03	-	1.75E-03	-	6.84E-04	-
20	1.47E-03	1.94	2.16E-04	3.02	9.67E-05	2.82
40	3.79E-04	1.96	2.69E-05	3.01	1.30E-05	2.90
80	9.61E-05	1.98	3.36E-06	3.00	1.68E-06	2.95
	e_w		$\bar{e}_w$		$e_w^-(x_{j+1/2})$	
10	8.94E-03	-	1.05E-03	-	1.12E-03	-
20	2.22E-03	2.01	1.36E-04	2.94	1.25E-04	3.17
40	5.53E-04	2.00	1.75E-05	2.96	1.47E-05	3.08
80	1.38E-04	2.00	2.22E-06	2.98	1.79E-06	3.04

Table 4.10: Example 2 when using P^2 polynomials on a uniform mesh of N cells. $T = 1$. The diffusion fluxes are chosen as (3.9).

	e_u		$\bar{e}_u$		$e_u^+(x_{j-1/2})$	
N	L^2 error	order	L^2 error	order	L^2error	order
10	2.94E-04	-	5.42E-05	-	5.42E-06	-
20	3.80E-05	2.95	3.41E-06	3.99	1.61E-07	5.07
40	4.83E-06	2.97	2.14E-07	3.99	4.94E-09	5.02
80	6.09E-07	2.99	1.34E-08	4.00	1.51E-10	5.03
	e_w		$\bar{e}_w$		$e_w^-(x_{j+1/2})$	
10	4.45E-04	-	2.88E-05	-	6.88E-06	-
20	5.57E-05	3.00	1.97E-06	3.87	2.29E-07	4.91
40	6.96E-06	2.97	1.30E-07	3.93	7.43E-09	4.95
80	8.70E-07	3.00	8.30E-09	3.96	2.38E-10	4.96

Table 4.11: Example 2 when using P^3 polynomials on a uniform mesh of N cells. $T = 1$. The diffusion fluxes are chosen as (3.9).

	e_u		$\bar{e}_u$		$e_u^+(x_{j-1/2})$	
N	L^2 error	order	L^2 error	order	L^2error	order
5	1.76E-04	-	4.37E-05	-	1.92E-06	-
10	1.16E-05	3.92	1.39E-06	4.97	1.49E-08	7.01
20	7.41E-07	3.96	4.39E-08	4.99	1.19E-10	6.96
40	4.69E-08	3.98	1.38E-09	4.99	2.66E-13	8.81
	e_w		$\bar{e}_w$		$e_w^-(x_{j+1/2})$	
5	2.73E-04	-	2.14E-05	-	2.69E-06	-
10	1.72E-05	3.99	7.76E-07	4.79	1.76E-08	7.26
20	1.07E-06	4.00	2.61E-08	4.90	1.29E-10	7.09
40	6.72E-08	4.00	8.45E-10	4.95	2.39E-12	5.76

Example 3. We solve the convection-dominated problem

$$\begin{cases} u_t + u_x = 0.01u_{xx} \\ u(x,0) = \sin(x) \\ u(0,t) = u(2\pi,t). \end{cases}$$

The exact solution to this problem is

$$u(x,t) = e^{-0.01t}\sin(x-t).$$

We use the upwind flux for the convective term, and take the diffusion fluxes to be (3.8). The projections for u and q are taken as P_h^- and P_h^+, respectively. The numerical traces for this problem are $u_h^- - 0.1q_h^+$ and $0.1u_h^-$. From Tables 4.12 to 4.14, $(k+2)$-th order superconvergence are obtained for $\bar{e}_u$, $\bar{e}_q$ and the point errors u^- and q^+. The only difference compared to Example 2 is that we now need a more refined mesh to observe superconvergence for $\bar{e}_q$.

If we use (3.9) as the diffusion fluxes, then the numerical traces are $u_h^- - 0.1q_h^-$ and $0.1u_h^+$. Define $w = u - 0.1q = u - 0.01u_x$ and again denote $\bar{e}_w$ as the difference between w and $P_h^- w$. Tables 4.15 to 4.17 show the superconvergence of the traces as well as $\bar{e}_u$ and $\bar{e}_w$.

Table 4.12: Example 3 when using P^1 polynomials on a uniform mesh of N cells. $T = 1$. The diffusion fluxes are chosen as (3.8).

	e_u		$\bar{e}_u$		$e_u^-(x_{j+1/2})$	
N	L^2 error	order	L^2 error	order	L^2error	order
10	1.64E-02	-	3.47E-03	-	4.78E-03	-
20	4.18E-03	1.97	4.37E-04	2.99	5.82E-04	3.04
40	1.05E-03	1.99	5.38E-05	3.02	6.61E-05	3.14
80	2.63E-04	2.00	6.63E-06	3.02	7.13E-06	3.21
	e_q		$\bar{e}_q$		$e_q^+(x_{j-1/2})$	
160	4.17E-06	-	4.11E-06	-	7.06E-06	-
320	1.20E-06	1.79	6.40E-07	2.68	1.10E-06	2.68
640	3.43E-07	1.81	9.13E-08	2.81	1.57E-07	2.81
1280	9.33E-08	1.88	1.23E-08	2.89	2.11E-08	2.89

Table 4.13: Example 3 when using P^2 polynomials on a uniform mesh of N cells. $T = 1$. The diffusion fluxes are chosen as (3.8).

	e_u		$\bar{e}_u$		$e_u^-(x_{j+1/2})$	
N	L^2 error	order	L^2 error	order	L^2error	order
10	8.43E-04	-	7.16E-05	-	3.12E-05	-
20	3.94E-05	3.00	1.40E-06	3.89	1.48E-07	4.92
40	4.92E-06	3.00	9.17E-08	3.93	4.75E-09	4.96
80	6.15E-07	3.00	5.87E-09	3.96	1.51E-10	4.98
	e_q		$\bar{e}_q$		$e_q^+(x_{j-1/2})$	
160	1.68E-08	-	1.58E-08	-	1.10E-08	-
320	2.18E-09	2.95	1.14E-09	3.79	4.50E-10	4.61
640	2.92E-10	2.90	7.46E-11	3.93	1.58E-11	4.83
1280	3.83E-11	2.93	2.97E-12	4.65	4.48E-13	5.14

Table 4.14: Example 3 when using P^3 polynomials on a uniform mesh of N cells. $T = 1$. The diffusion fluxes are chosen as (3.8).

	e_u		$\bar{e}_u$		$e_u^-(x_{j+1/2})$	
N	L^2 error	order	L^2 error	order	L^2error	order
5	5.24E-04	-	7.53E-05	-	9.75E-05	-
10	3.36E-05	3.96	2.48E-06	4.93	1.88E-06	5.70
20	2.05E-06	4.04	4.47E-08	5.79	4.97E-08	5.24
40	1.28E-07	3.98	1.24E-09	5.17	1.86E-09	4.74
	e_q		$\bar{e}_q$		$e_q^+(x_{j-1/2})$	
80	6.19E-10	-	6.12E-10	-	5.07E-10	-
160	4.07E-11	3.93	2.59E-11	4.56	8.31E-12	5.93
320	2.74E-12	3.89	9.29E-13	4.80	9.00E-14	6.53

Table 4.15: Example 3 when using P^1 polynomials on a uniform mesh of N cells. $T = 1$. The diffusion fluxes are chosen as (3.9).

	e_u		$\bar{e}_u$		$e_u^+(x_{j-1/2})$	
N	L^2 error	order	L^2 error	order	L^2error	order
160	4.17E-05	-	4.11E-05	-	7.06E-05	-
320	1.20E-05	1.79	6.40E-06	2.68	1.10E-05	2.68
640	3.43E-06	1.81	9.13E-07	2.81	1.57E-06	2.81
	e_w		$\bar{e}_w$		$e_w^-(x_{j+1/2})$	
10	1.64E-02	-	3.49E-03	-	4.80E-03	-
20	4.18E-03	1.97	4.39E-04	2.99	5.83E-04	3.04
40	1.05E-03	1.99	5.39E-05	3.02	6.63E-05	3.14
80	2.63E-04	2.00	6.64E-06	3.02	7.14E-06	3.21

Table 4.16: Example 3 when using P^2 polynomials on a uniform mesh of N cells. $T = 1$. The diffusion fluxes are chosen as (3.9).

	e_u		$\bar{e}_u$		$e_u^+(x_{j-1/2})$	
N	L^2 error	order	L^2 error	order	L^2error	order
160	1.68E-07	-	1.58E-07	-	1.10E-07	-
320	2.18E-08	2.95	1.14E-08	3.79	4.50E-09	4.61
640	2.92E-09	2.90	7.50E-10	3.92	1.58E-10	4.83
	e_w		$\bar{e}_w$		$e_w^-(x_{j+1/2})$	
10	8.43E-04	-	7.13E-05	-	3.21E-05	-
20	1.06E-04	3.00	4.59E-06	3.96	2.58E-06	3.63
40	1.32E-05	3.00	2.75E-07	4.06	2.68E-07	3.27
80	1.65E-06	3.00	1.27E-08	4.44	2.03E-08	3.72

Table 4.17: Example 3 when using P^3 polynomials on a uniform mesh of N cells. $T = 1$. The diffusion fluxes are chosen as (3.9).

	e_u		$\bar{e}_u$		$e_u^+(x_{j-1/2})$	
N	L^2 error	order	L^2 error	order	L^2error	order
80	6.19E-09	-	6.12E-09	-	5.07E-09	-
160	4.07E-10	3.93	2.59E-10	4.56	8.31E-11	5.93
320	2.74E-11	3.89	9.38E-12	4.79	1.61E-12	5.69
	e_w		$\bar{e}_w$		$e_w^-(x_{j+1/2})$	
5	5.23E-04	-	7.35E-05	-	9.56E-05	-
10	3.35E-05	3.96	2.45E-06	4.91	1.94E-06	5.62
20	2.05E-06	4.03	4.46E-08	5.78	4.95E-08	5.29
40	1.28E-07	4.00	1.24E-09	5.17	1.86E-09	4.73

4.2 Linear equations with variable coefficients

In this subsection, linear equations with variable coefficients are discussed. The coefficient for the convection term can depend on x.

Example 4. We solve the convection-diffusion equation with a variable coefficient in the convective term

$$\begin{cases} u_t + (a(x)u)_x = u_{xx} + c(x,t) \\ u(x,0) = \sin(x) \\ u(0,t) = u(2\pi,t) \end{cases} \tag{4.1}$$

where $a(x)$ and $c(x,t)$ are given by

$$\begin{aligned} a(x) &= \sin(x) + 2, \\ c(x,t) &= e^{-t}(\cos(x)\sin(x-t) + \cos(x-t)(1+\sin(x))). \end{aligned}$$

The exact solution to this problem is

$$u(x,t) = e^{-t}\sin(x-t).$$

Since $a(x) > 0$, we will use u_h^- as the convection flux. If the diffusion fluxes are chosen as (3.8), the numerical traces are $a(x)u_h^- - q_h^+$ and u_h^-. From Tables 4.18 to 4.20, we clearly see superconvergence for $\bar{e}_u$, $\bar{e}_q$ as well as the point errors for u_h^- and q_h^+, which imply the superconvergence of the numerical traces. The results are similar to the constant coefficient case in

Example 2.

Table 4.18: Example 4 when using P^1 polynomials on a uniform mesh of N cells. $T = 1$. The diffusion fluxes are chosen as (3.8).

	e_u		$\bar{e}_u$		$e_u^-(x_{j+1/2})$	
N	L^2 error	order	L^2 error	order	L^2error	order
10	6.47E-03	-	1.31E-03	-	1.61E-03	-
20	1.58E-03	2.04	1.73E-04	2.92	2.02E-04	3.00
40	3.92E-04	2.01	2.25E-05	2.95	2.54E-05	2.99
80	9.77E-05	2.00	2.87E-06	2.97	3.20E-06	2.99
	e_q		$\bar{e}_q$		$e_q^+(x_{j-1/2})$	
10	5.56E-03	-	2.33E-03	-	1.54E-03	-
20	1.45E-03	1.94	3.01E-04	2.95	2.06E-04	2.90
40	3.74E-04	1.95	3.84E-05	2.97	2.71E-05	2.93
80	9.54E-05	1.97	4.86E-06	2.98	3.50E-06	2.96

On the other hand, if the diffusive fluxes are taken as (3.9), then the numerical traces are $a(x)u_h^- - q_h^-$ and u_h^+. Define $w = a(x)u - q$. In this case, we define the projection for u as P_h^+ and $e_w^-(x_{j+\frac{1}{2}}) = a(x)u^- - q^- - w$. From Table 4.21, we have superconvergence for $\bar{e}_u$, $e_u^+(x_{j-1/2})$ and $e_w^-(x_{j+\frac{1}{2}})$.

Example 5. We solve the equation (4.1) with

$$\begin{aligned} a(x) &= \sin(x), \\ c(x,t) &= e^{-t}(\cos(x)\sin(x-t) + \cos(x-t)(\sin(x) - 1)). \end{aligned}$$

The exact solution to this problem is still

$$u(x,t) = e^{-t}\sin(x-t).$$

Table 4.19: Example 4 when using P^2 polynomials on a uniform mesh of N cells. $T = 1$. The diffusion fluxes are chosen as (3.8).

	e_u		$\bar{e}_u$		$e_u^-(x_{j+1/2})$	
N	L^2 error	order	L^2 error	order	L^2error	order
10	3.15E-04	-	1.92E-05	-	6.95E-06	-
20	3.94E-05	3.00	1.34E-06	3.85	2.28E-07	4.93
40	4.92E-06	3.00	8.94E-08	3.90	7.35E-09	4.96
80	6.15E-07	3.00	5.80E-09	3.95	2.34E-10	4.98
	e_q		$\bar{e}_q$		$e_q^+(x_{j-1/2})$	
10	2.86E-04	-	8.09E-05	-	2.06E-05	-
20	3.74E-05	2.94	5.26E-06	3.94	6.80E-07	4.92
40	4.79E-06	2.96	3.34E-07	3.98	2.19E-08	4.96
80	6.07E-07	2.98	2.11E-08	3.99	6.96E-10	4.98

In this example, $a(x)$ is no longer always positive. However, we can still use the upwind flux, namely, if $a(x_{j+\frac{1}{2}}) > 0$, then at $x_{j+\frac{1}{2}}$, we use u_h^-; otherwise, we use u_h^+.

If the diffusion fluxes are taken as (3.8), then the numerical traces are $a(x)\hat{u_h} - q_h^+$ and u_h^-. Define $w = a(x)u - q$ and $e_w = a(x)\hat{u_h} - q_h^+ - w$, and take the projection for u as $P_h^- u$. From Table 4.22, superconvergence for the numerical traces and the projection for u are achieved. Likewise, if the diffusion fluxes are taken as (3.9), then the numerical traces are $w = a(x)\hat{u_h} - q_h^-$ and u_h^+. From Table 4.23, we observe similar superconvergence results.

Table 4.20: Example 4 when using P^3 polynomials on a uniform mesh of N cells. $T = 1$. The diffusion fluxes are chosen as (3.8).

	e_u		$\bar{e}_u$		$e_u^-(x_{j+1/2})$	
N	L^2 error	order	L^2 error	order	L^2error	order
5	1.93E-04	-	1.51E-05	-	4.49E-06	-
10	1.21E-05	3.99	5.24E-07	4.85	4.32E-08	6.70
20	7.60E-07	4.00	1.79E-08	4.87	3.52E-10	6.94
40	4.75E-08	4.00	5.88E-10	4.93	3.41E-12	6.69
	e_q		$\bar{e}_q$		$e_q^+(x_{j-1/2})$	
5	1.73E-04	-	6.83E-05	-	1.31E-05	-
10	1.14E-05	3.93	2.34E-06	4.87	1.08E-07	6.92
20	7.34E-07	3.96	7.57E-08	4.95	8.84E-10	6.94
40	4.66E-08	3.98	2.40E-09	4.98	7.68E-12	6.85

Table 4.21: Example 4 on a uniform mesh of N cells. $T = 1$. The diffusion fluxes are chosen as (3.9).

		e_u		$\bar{e}_u$		$e_u^+(x_{j-1/2})$		$e_w^-(x_{j+\frac{1}{2}})$	
	N	L^2 error	order	L^2 error	order	L^2error	order	L^2error	order
P^1	10	5.36E-03	-	2.98E-03	-	2.14E-03	-	2.88E-03	-
	20	1.41E-03	1.93	3.81E-04	2.97	2.94E-04	2.87	3.42E-04	3.08
	40	3.68E-04	1.93	4.84E-05	2.98	3.91E-05	2.91	4.17E-05	3.04
	80	9.46E-05	1.96	6.12E-06	2.99	5.06E-06	2.95	5.15E-06	3.02
P^2	N	L^2 error	order	L^2 error	order	L^2error	order	L^2error	order
	10	2.79E-04	-	1.00E-04	-	2.67E-05	-	8.65E-06	-
	20	3.68E-05	2.92	6.56E-06	3.93	9.17E-07	4.87	3.14E-07	4.78
	40	4.75E-06	2.95	4.18E-07	3.97	2.99E-08	4.94	1.06E-08	4.88
	80	6.04E-07	2.98	2.63E-08	3.99	9.54E-10	4.97	3.50E-10	4.93
P^3	N	L^2 error	order	L^2 error	order	L^2error	order	L^2error	order
	5	1.65E-04	-	7.49E-05	-	1.44E-05	-	8.96E-06	-
	10	1.11E-05	3.89	2.55E-06	4.88	1.34E-07	6.75	8.60E-08	6.70
	20	7.24E-07	3.94	8.28E-08	4.95	1.13E-09	6.89	7.42E-10	6.86
	40	4.63E-08	3.97	2.63E-09	4.98	9.88E-12	6.84	8.28E-12	6.49

Table 4.22: Example 5 on a uniform mesh of N cells. $T = 1$. The diffusion fluxes are chosen as (3.8).

		e_u		$\bar{e}_u$		$e_u^-(x_{j+1/2})$		$e_w(x_{j+1/2})$	
	N	L^2 error	order	L^2 error	order	L^2error	order	L^2error	order
P^1	10	6.12E-03	-	1.55E-03	-	7.53E-04	-	1.43E-03	-
	20	1.54E-03	1.99	1.98E-04	2.97	9.14E-05	3.04	1.84E-04	2.96
	40	3.87E-04	1.99	2.49E-05	2.99	1.13E-05	3.01	2.34E-05	2.98
	80	9.72E-05	1.99	3.13E-06	2.99	1.41E-06	3.01	2.95E-06	2.99
P^2	N	L^2 error	order	L^2 error	order	L^2error	order	L^2error	order
	10	3.09E-04	-	2.79E-05	-	6.75E-06	-	3.17E-06	-
	20	3.89E-05	2.99	1.90E-06	3.88	2.09E-07	5.01	1.06E-07	4.91
	40	4.89E-06	2.99	1.24E-07	3.93	6.53E-09	5.00	3.45E-09	4.93
	80	6.13E-07	3.00	7.95E-09	3.97	2.04E-10	5.00	1.11E-10	4.96
P^3	N	L^2 error	order	L^2 error	order	L^2error	order	L^2error	order
	5	1.86E-04	-	2.98E-05	-	3.64E-06	-	3.27E-06	-
	10	1.20E-05	3.99	9.39E-07	4.99	2.47E-08	7.20	2.09E-08	7.29
	20	7.54E-07	3.99	2.92E-08	5.00	1.92E-10	7.01	1.55E-10	7.08
	40	4.73E-08	3.99	9.14E-10	5.00	1.45E-12	7.02	1.43E-12	6.76

Table 4.23: Example 5 on a uniform mesh of N cells. $T = 1$. The diffusion fluxes are chosen as (3.9).

		e_u		$\bar{e}_u$		$e_u^-(x_{j+1/2})$		$e_w(x_{j+1/2})$	
	N	L^2 error	order	L^2 error	order	L^2error	order	L^2error	order
P^1	10	6.14E-03	-	9.37E-04	-	5.37E-04	-	1.21E-03	-
	20	1.54E-03	1.99	1.17E-04	3.01	6.68E-05	3.01	1.49E-04	3.02
	40	3.88E-04	1.99	1.47E-05	2.99	8.49E-06	2.98	1.86E-05	3.00
	80	9.72E-05	1.99	1.84E-06	2.99	1.08E-06	2.98	2.33E-06	3.00
	N	L^2 error	order	L^2 error	order	L^2error	order	L^2error	order
P^2	10	3.07E-04	-	4.06E-05	-	5.08E-06	-	4.04E-06	-
	20	3.88E-05	2.98	2.51E-06	4.02	1.46E-07	5.12	1.17E-07	5.12
	40	4.89E-06	2.99	1.56E-07	4.01	4.45E-09	5.04	3.54E-09	5.04
	80	6.13E-07	3.00	9.73E-09	4.00	1.37E-10	5.02	1.10E-10	5.01
	N	L^2 error	order	L^2 error	order	L^2error	order	L^2error	order
P^2	5	1.90E-04	-	2.85E-05	-	3.60E-06	-	2.85E-06	-
	10	1.20E-05	3.98	7.63E-07	5.22	1.64E-08	7.77	1.85E-08	7.27
	20	7.55E-07	3.99	2.34E-08	5.03	1.24E-10	7.06	1.37E-10	7.08
	40	4.73E-08	4.00	7.31E-10	5.00	1.43E-12	6.43	1.06E-12	7.01

4.3 Nonlinear equations

In this subsection, general nonlinear equations are discussed.

Example 6. We solve the equation with a nonlinear convective term

$$\begin{cases} u_t + (u^3)_x = u_{xx} + c(x,t) \\ u(x,0) = \sin(x) \\ u(0,t) = u(2\pi,t) \end{cases}$$

with

$$c(x,t) = -e^{-3t}\cos(x-t)(e^{2t} - 3\sin^2(x-t))).$$

The exact solution to this problem is

$$u(x,t) = e^{-t}\sin(x-t).$$

Since $f'(u) = u^2 \geq 0$, we can simply use the upwind convection flux. If we use (3.8) as the diffusion fluxes, the numerical traces are $(u_h^-)^3 - \hat{q}_h$ and $\hat{u}_h$. The numerical errors and orders are listed in Tables 4.24 to 4.26. Superconvergence conclusions are similar to those in Examples 2 and 4 for the linear equations.

If the diffusion fluxes are taken as (3.9), then the numerical traces are u_h^+ and $(u_h^-)^3 - q_h^-$. By defining $w = u^3 - q$, we have superconvergence for $\bar{e}_u$, u_h^+ and w_h^-, as observed in Table 4.27.

Table 4.24: Example 6 when using P^1 polynomials on a uniform mesh of N cells. $T = 1$. The diffusion fluxes are chosen as (3.8).

	e_u		$\bar{e}_u$		$e_u^-(x_{j+1/2})$	
N	L^2 error	order	L^2 error	order	L^2error	order
10	6.34E-03	-	1.29E-03	-	1.03E-03	-
20	1.57E-03	2.01	1.69E-04	2.93	1.22E-04	3.08
40	3.91E-04	2.00	2.17E-05	2.97	1.48E-05	3.04
80	9.77E-05	2.00	2.74E-06	2.98	1.83E-06	3.02
	e_q		$\bar{e}_q$		$e_q^+(x_{j-1/2})$	
10	5.92E-03	-	1.31E-03	-	9.89E-04	-
20	1.51E-03	1.97	1.65E-04	2.99	1.22E-04	3.02
40	3.83E-04	1.98	2.06E-05	3.00	1.53E-05	3.00
80	9.67E-05	1.99	2.58E-06	3.00	1.92E-06	2.99

Example 7. We solve the following equation

$$\begin{cases} u_t + (u^2)_x = u_{xx} + c(x,t) \\ u(x,0) = \sin(x) \\ u(0,t) = u(2\pi,t) \end{cases}$$

with

$$c(x,t) = -e^{-2t}\cos(x-t)(e^t - 2\sin(x-t))).$$

The exact solution to this problem is

$$u(x,t) = e^{-t}\sin(x-t).$$

This time the wind direction for the convective term changes and we use the Godunov flux [13] for the convection. The diffusive fluxes are chosen as

Table 4.25: Example 6 when using P^2 polynomials on a uniform mesh of N cells. $T = 1$. The diffusion fluxes are chosen as (3.8).

	e_u		$\bar{e}_u$		$e_u^-(x_{j+1/2})$	
N	L^2 error	order	L^2 error	order	L^2error	order
10	3.15E-04	-	2.31E-05	-	3.38E-06	-
20	3.94E-05	3.00	1.48E-06	3.96	9.73E-08	5.12
40	4.92E-06	3.00	9.43E-08	3.97	2.96E-09	5.04
80	6.15E-07	3.00	5.96E-09	3.99	9.07E-11	5.03
	e_q		$\bar{e}_q$		$e_q^+(x_{j-1/2})$	
10	3.05E-04	-	3.52E-05	-	3.50E-06	-
20	3.87E-05	2.98	2.20E-06	4.00	9.65E-08	5.18
40	4.88E-06	2.99	1.38E-07	4.00	2.95E-09	5.03
80	6.12E-07	2.99	8.63E-09	4.00	9.14E-11	5.01

(3.8) and the numerical traces are $\hat{u_h^2} - q_h^+$ and u_h^-. Define $w = u^2 - q$. The results are listed in Table 4.28. We note that the superconvergence conclusion is similar to the linear case in Example 5. The results for the diffusive fluxes (3.9) are similar and hence omitted here.

Example 8. We solve the following equation

$$\begin{cases} u_t = (b(u)u_x)_x + c(x,t) \\ u(x,0) = \sin(x) \\ u(0,t) = u(2\pi,t) \end{cases}$$

Table 4.26: Example 6 when using P^3 polynomials on a uniform mesh of N cells. $T = 1$. The diffusion fluxes are chosen as (3.8).

	e_u		$\bar{e}_u$		$e_u^-(x_{j+1/2})$	
N	L^2 error	order	L^2 error	order	L^2error	order
5	1.93E-04	-	1.72E-05	-	3.57E-06	-
10	1.21E-05	3.99	5.68E-07	4.92	1.62E-08	7.78
20	7.60E-07	4.00	1.87E-08	4.93	1.21E-10	7.07
40	4.75E-08	4.00	6.01E-10	4.96	9.58E-13	6.98
	e_q		$\bar{e}_q$		$e_q^+(x_{j-1/2})$	
5	1.80E-04	-	4.41E-05	-	7.77E-06	-
10	1.17E-05	3.95	1.36E-06	5.02	2.94E-08	8.04
20	7.44E-07	3.96	4.20E-08	5.01	2.10E-10	7.13
40	4.70E-08	3.98	1.31E-09	5.01	1.58E-12	7.05

with

$$\begin{aligned} b(u) &= u^4, \\ c(x,t) &= -e^{-5t}(e^{4t}\cos(t-x) - e^{4t}\sin(t-x) \\ &- 4\cos^2(t-x)\sin^3(t-x) + \sin^5(t-x)). \end{aligned}$$

This is a nonlinear diffusion equation. The exact solution to this problem is

$$u(x,t) = e^{-t}\sin(x-t).$$

In the computation below, we use the diffusion fluxes (2.3) with $a(u) = u^2$ and $g(u) = u^3/3$. The numerical traces are $w_1 = \frac{[g(u_h)]}{[u_h]} q_h^+$ and $w_2 = g(u_h^-)$. The errors for w_1 and w_2 are $e_{w_1} = w_1 - a(u)q = w_1 - u^4 u_x$, $e_{w_2} = w_2 - g(u) =$

Table 4.27: Example 6 on a uniform mesh of N cells. $T = 1$. The diffusion fluxes are chosen as (3.9).

		e_u		$\bar{e}_u$		$e_u^+(x_{j-1/2})$		$e_w^-(x_{j+1/2})$	
	N	L^2 error	order	L^2 error	order	L^2error	order	L^2 error	order
P^1	10	6.10E-03	-	1.31E-03	-	5.00E-04	-	1.65E-03	-
	20	1.54E-03	1.99	1.68E-04	2.96	5.45E-05	3.20	2.03E-04	3.02
	40	3.87E-04	1.99	2.14E-05	2.98	6.29E-06	3.11	2.54E-05	3.00
	80	9.72E-05	1.99	2.70E-06	2.99	7.55E-07	3.06	3.18E-06	3.00
	N	L^2 error	order	L^2 error	order	L^2error	order	L^2 error	order
P^2	10	3.13E-04	-	3.07E-05	-	7.35E-06	-	1.88E-06	-
	20	3.92E-05	2.99	1.75E-06	4.14	2.12E-07	5.11	4.47E-08	5.40
	40	4.91E-06	3.00	1.04E-07	4.06	6.35E-09	5.06	1.43E-09	4.97
	80	6.14E-07	3.00	6.39E-09	4.03	1.95E-10	5.03	4.83E-11	4.88
	N	L^2 error	order	L^2 error	order	L^2error	order	L^2 error	order
P^3	5	1.87E-04	-	2.36E-05	-	2.82E-06	-	7.34E-06	-
	10	1.20E-05	3.97	7.37E-07	5.00	1.48E-08	7.57	3.52E-08	7.71
	20	7.54E-07	3.99	2.32E-08	4.99	1.17E-10	6.99	2.48E-10	7.15
	40	4.73E-08	3.99	7.31E-10	4.99	4.64E-13	7.97	2.76E-12	6.49

$w_2 - u^3/3$. From Table 4.29, we observe that w_1 and w_2 are superconvergent of order $(k + 2)$.

Example 9. We solve the following equation

$$\begin{cases} u_t + (u^2)_x = (b(u)u_x)_x + c(x,t) \\ u(x,0) = \sin(x) \\ u(0,t) = u(2\pi,t) \end{cases}$$

Table 4.28: Example 7 on a uniform mesh of N cells. $T = 1$. The diffusion fluxes are chosen as (3.8).

		e_u		$\bar{e}_u$		$e_u^-(x_{j+1/2})$		$e_w(x_{j+1/2})$	
	N	L^2 error	order	L^2 error	order	L^2error	order	L^2error	order
	10	6.10E-03	-	1.56E-03	-	8.92E-04	-	1.53E-03	-
P^1	20	1.54E-03	1.99	2.02E-04	2.95	1.08E-04	3.05	1.96E-04	2.97
	40	3.87E-04	1.99	2.58E-05	2.97	1.33E-05	3.02	2.48E-05	2.98
	80	9.72E-05	1.99	3.25E-06	2.98	1.66E-06	3.01	3.13E-06	2.99
	N	L^2 error	order	L^2 error	order	L^2error	order	L^2error	order
	10	3.11E-04	-	2.73E-05	-	5.56E-06	-	5.29E-06	-
P^2	20	3.91E-05	2.99	1.71E-06	4.00	1.68E-07	5.05	1.60E-07	5.05
	40	4.91E-06	3.00	1.07E-07	3.99	5.17E-09	5.02	5.07E-09	4.98
	80	6.14E-07	3.00	6.75E-09	3.99	1.61E-10	5.01	1.60E-10	4.98
	N	L^2 error	order	L^2 error	order	L^2error	order	L^2error	order
	5	1.88E-04	-	2.27E-05	-	2.84E-06	-	6.32E-06	-
P^3	10	1.20E-05	3.97	7.59E-07	4.90	2.16E-08	7.04	2.70E-08	7.87
	20	7.54E-07	3.99	2.51E-08	4.92	1.63E-10	7.05	2.02E-10	7.06
	40	4.73E-08	3.99	8.09E-10	4.96	1.27E-12	7.01	1.34E-12	7.24

with

$$\begin{aligned} b(u) &= u^4, \\ c(x,t) &= -e^{-5t}(e^{4t}\cos(t-x) - e^{4t}\sin(t-x) \\ &\quad -4\cos^2(t-x)\sin^3(t-x) + \sin^5(t-x) + e^{3t}\sin(2(t-x))). \end{aligned}$$

This is a convection diffusion equation which is nonlinear in both convection and diffusion, and the wind direction for the convection term changes sign. Therefore, this is the most general example given in this paper. The exact

Table 4.29: Example 8 on a uniform mesh of N cells. $T = 1$.

		e_u		e_q		$e_{w_1}(x_{j+1/2})$		$e_{w_2}(x_{j+1/2})$	
	N	L^2 error	order	L^2 error	order	L^2error	order	L^2error	order
P^1	10	7.36E-03	-	2.49E-03	-	5.61E-04	-	4.60E-04	-
	20	1.80E-03	2.03	6.91E-04	1.85	1.03E-04	2.44	6.47E-05	2.83
	40	4.39E-04	2.03	2.40E-04	1.53	2.07E-05	2.32	1.11E-05	2.55
	80	1.04E-04	2.07	5.98E-05	2.00	3.14E-06	2.72	1.32E-06	3.07
	N	L^2 error	order	L^2 error	order	L^2error	order	L^2error	order
P^2	10	7.07E-04	-	3.54E-04	-	1.97E-05	-	4.10E-05	-
	20	6.24E-05	3.50	4.46E-05	2.99	4.76E-06	2.06	2.13E-06	4.26
	40	6.09E-06	3.36	5.23E-06	3.09	3.20E-07	3.89	1.13E-07	4.24
	80	6.75E-07	3.17	6.09E-07	3.10	1.47E-08	4.44	4.41E-09	4.67
	N	L^2 error	order	L^2 error	order	L^2error	order	L^2error	order
P^3	5	1.08E-03	-	6.15E-04	-	6.11E-05	-	6.29E-05	-
	10	2.92E-05	5.21	3.43E-05	4.16	3.03E-06	4.33	1.71E-06	5.20
	20	1.19E-06	4.61	2.07E-06	4.05	7.46E-08	5.34	5.15E-08	5.06

solution to this problem is

$$u(x,t) = e^{-t}\sin(x-t).$$

We use the Godunov flux for the convection term, and (2.3) for the diffusion fluxes. The numerical traces are $w_1 = \hat{u_h^2} - \frac{[g(u_h)]}{[u_h]} q_h^+$ and $w_2 = g(u_h^-)$. The errors for w_1 and w_2 are $e_{w_1} = w_1 - u^2 + a(u)q = w_1 - u^2 + u^4 u_x$ and $e_{w_2} = w_2 - g(u) = w_2 - u^3/3$. The results are listed in Table 4.30. We clearly observe $(k+2)$-th order superconvergence.

Table 4.30: Example 9 on a uniform mesh of N cells. $T = 1$.

		e_u		e_q		$e_{w_1}(x_{j+1/2})$		$e_{w_2}(x_{j+1/2})$	
	N	L^2 error	order	L^2 error	order	L^2error	order	L^2error	order
	20	1.47E-03	-	2.50E-03	-	2.96E-04	-	2.31E-04	-
P^1	40	3.42E-04	2.10	9.96E-04	1.33	3.74E-05	2.98	4.51E-05	2.35
	80	8.36E-05	2.03	3.58E-04	1.48	5.04E-06	2.89	8.08E-06	2.48
	N	L^2 error	order	L^2 error	order	L^2error	order	L^2error	order
	10	5.26E-04	-	3.24E-04	-	2.33E-04	-	6.10E-05	-
P^2	20	5.99E-05	3.13	5.71E-05	2.51	2.50E-05	3.22	5.57E-06	3.45
	40	6.05E-06	3.31	9.60E-06	2.57	1.28E-06	4.29	3.77E-07	3.88
	80	6.73E-07	3.17	1.68E-06	2.52	7.03E-08	4.18	2.87E-08	3.71
	N	L^2 error	order	L^2 error	order	L^2error	order	L^2error	order
	5	4.07E-04	-	3.78E-04	-	1.23E-04	-	3.15E-05	-
P^3	10	1.61E-05	4.66	3.18E-05	3.57	4.59E-06	4.74	2.39E-06	3.72
	20	7.42E-07	4.44	2.51E-06	3.66	7.80E-08	5.88	8.38E-08	4.84
	40	4.43E-08	4.07	1.99E-07	3.66	2.50E-09	4.96	2.63E-09	4.99

4.4 Summary

In this subsection, we summarize the results for the numerical tests in this section. For the general convection diffusion equation (1.1), we have various convergence behaviors based on f and b.

Case A. $f'(u) \geq 0$, $b(u)$ is a nonzero constant.

In this case, the convection flux is $f(u_h^-, x)$. If the diffusion fluxes are taken consistently as (3.8), that is, if u_h^- is used both for the convective flux and for the diffusive flux, then we have superconvergence for u and q in the sense of both projection errors and point errors. If the diffusion fluxes are taken as (3.9), we have superconvergence for u in point errors and projection errors, and superconvergence for point errors of the other numerical trace $f(u_h^-) - \sqrt{b}q_h^-$. Moreover, if f is a linear function of u, then the projection errors for $f(u_h^-) - \sqrt{b}q_h^-$ is also superconvergent.

Case B. General f, $b(u)$ is a nonzero constant.

In this case, if we take the diffusion fluxes as (3.8), we have superconvergence for u in the sense of both projection errors and point errors. The other numerical trace $\hat{f}(u_h) - \sqrt{b}q_h^-$ is also superconvergent. The conclusion is similar for the other choice of the diffusion fluxes (3.9).

Case C. $b(u)$ is nonlinear.

In this case, we have superconvergence in point errors for the two numerical traces.

Case D. $b = 0$.

These are the pure convection equations, and fall into the discussion in [6].

To summarize, the numerical traces are always superconvergent. In some cases, the traces may coincide with u or q or their linear combinations. Then the corresponding projection error will also be superconvergent.

5 Conclusions and future work

In this paper, we have studied the convergence behavior of the LDG methods for convection-diffusion equations when the alternating fluxes are used. We prove that the numerical solution will be superconvergent towards a particular projection of the exact solution for the heat equation in the case of P^1. Numerical tests are given to demonstrate that superconvergence can be observed in many more cases. For general equations, the relationship between superconvergence and the numerical fluxes are shown. The numerical traces are always superconvergent in our examples. To obtain superconvergence in projection errors, if there is a preferred wind direction for the convection term, it is better to take the diffusion flux for u from the same side.

Future work includes the proof of superconvergence for general P^k polynomials for the heat equation and the exploration of higher-order nonlinear equations.

6 Acknowledgement

Research of the second author is supported by NSF grant DMS-0510345.

References

[1] Adjerid S, Devine K, Flaherty J, Krivodonova L. A posteriori error estimation for discontinuous Galerkin solutions of hyperbolic problems.

Computational Methods in Applied Mechanics and Engineering 2002; 191: 1097–1112.

[2] Adjerid S, Klauser A. Superconvergence of discontinuous finite element solutions for transient convection-diffusion problems. Journal of Scientific Computing 2005; 22/23: 5–24.

[3] Adjerid S, Massey T. Superconvergence of discontinuous Galerkin solutions for a nonlinear scalar hyperbolic problem. Computational Methods in Applied Mechanics and Engineering 2006; 195: 3331–3346.

[4] Bassi F, Rebay S. A high-order accurate discontinuous finite element method for the numerical solution of the compressible Navier-Stokes equations. Journal of Computational Physics 1997; 131: 267–279.

[5] Celiker F, Cockburn B. Superconvergence of the numerical traces of discontinuous Galerkin and hybridized methods for convection-diffusion problems in one space dimension. Mathematics of Computation 2007; 76: 67–96.

[6] Cheng Y, Shu C-W. Superconvergence and time evolution of discontinuous Galerkin finite element solutions. Preprint submitted to Journal of Computational Physics.

[7] Cockburn B, Hou S, Shu C-W. The Runge-Kutta local projection discontinuous Galerkin finite element method for conservation laws IV: the multidimensional case. Mathematics of Computation 1990; 54: 545–581.

[8] Cockburn B, Lin S-Y, Shu C-W. TVB Runge-Kutta local projection discontinuous Galerkin finite element method for conservation laws III: one dimensional systems. Journal of Computational Physics 1989; 84: 90–113.

[9] Cockburn B, Shu C-W. TVB Runge-Kutta local projection discontinuous Galerkin finite element method for conservation laws II: general framework. Mathematics of Computation 1989; 52: 411–435.

[10] Cockburn B, Shu C-W. The Runge-Kutta local projection P1-discontinuous Galerkin finite element method for scalar conservation laws. Mathematical Modelling and Numerical Analysis 1991; 25: 337–361.

[11] Cockburn B, Shu C-W. The Runge-Kutta discontinuous Galerkin method for conservation laws V: multidimensional systems. Journal of Computational Physics 1998; 141: 199–224.

[12] Cockburn B, Shu C-W. The local discontinuous Galerkin method for time-dependent convection-diffusion systems. SIAM Journal on Numerical Analysis 1998: 35: 2440–2463.

[13] LeVeque RJ. Numerical Methods for Conservation Laws. Birkhauser Verlag, Basel, 1990.

[14] Shu C-W, Osher S. Efficient implementation of essentially non-oscillatory shock-capturing schemes. Journal of Computational Physics 1988; 77: 439–471.

[15] Zhang M-P, Shu C-W. An analysis of three different formulations of the discontinuous Galerkin method for diffusion equations. Mathematical Models and Methods in Applied Sciences 2003; 13: 395–413.

[16] Zhang M-P, Shu C-W. An analysis of and a comparison between the discontinuous Galerkin and the spectral finite volume methods. Computers and Fluids 2005; 34: 581–592.

[17] Zhang Q, Shu C-W. Error estimates to smooth solutions of Runge-Kutta discontinuous Galerkin methods for scalar conservation laws. SIAM Journal on Numerical Analysis 2004; 42: 641–666.